Structural and Dynamic Properties of $(SiO_2)_6$ Silica Nanostructures: A Quantum Molecular Dynamics Study

Aiguo Zhong,[†] Chunying Rong,[‡] and Shubin Liu*,[‡,§]

Department of Chemistry, Taizhou College, Linhai, Zhejiang 317000, People's Republic of China, College of Chemistry and Chemical Engineering, Hunan Normal University, Changsha, Hunan 410081, People's Republic of China, and Divison of Research Computing, Information Technology Services, University of North Carolina, Chapel Hill, North Carolina 27599-3455

Received: January 10, 2007; In Final Form: February 13, 2007

Structural and dynamic properties of the building block of silica nanowires, $(SiO_2)_6$, are investigated by Born−Oppenheimer quantum molecular dynamics simulations. Thirteen conformers have been identified, seven of which have not been reported before. The energy component analysis shows that the lower electrostatic interaction differentiates the global minimum from the other structures. We also observe that the maximum hardness principle can be employed to justify the molecular stability for this system. Time profiles of a few density functional reactivity indices exhibit correlations of dynamic fluctuations between HOMO and LUMO and between chemical potential and hardness. Electrophilicity, nucleaofugality, and electrofugality indices are found to change concurrently and significantly, indicating that the nanostructures sampled during the dynamic process are exceedingly reactive and rich in chemistry.

1. Introduction

Silica nanowires have been of recent interest in the literature[1] because of their potential applications in photoluminescence, tailored drug-delivery miscroelectronics/catalysis, and fabricating nanoscale electronic and optoelectronic devices.[2−4] While extensive studies from both experimental and theoretical perspectives have been available,[5−10] many questions about their structural and dynamic properties still remain unanswered. For example, how are silica nanowires formed? Are they stable? How many metastable structures are accessible in gas phase? Are they chemically volatile? Unlike bulk silica, whose building unit is the silicon-centered corner-sharing SiO_4 tetrahedron forming scaffolds in terms of six-membered rings (6MR), silica chains assemble from edge-sharing two-membered rings (2MR), three-member rings (3MR), or four-membered-rings (4MR) terminated at each end by nonbridging oxygen.[5−10] These fundamental building blocks of the silica nanostructure can shuffle with each other generating a large number of conformations, many of which can be accessed during the synthetic and dynamic evolution processes.

Earlier, Harkless and co-workers[5] employed classical molecular dynamic simulations to search for stable/metastable nanostructures of SiO_2 clusters, but what they found was soon shown to be quite different from ab initio and density functional theory (DFT) results.[9] Flikkema and Bromley[8] later improved the interatomic potential and confirmed a few building blocks for nanoscale silica. Nevertheless, the lowest energy structures reported were still inconsistent with DFT/ab initio results. Very recently, Zhang and co-workers[9] applied pseudopotential and numerical basis set based ab initio molecular dynamics (AIMD) approach to silica nanowires and performed AIMD simulations

for 5 ps at 5000 K. More conformers have been discovered from the study. For instance, for $(SiO_2)_6$, a total of 6 conformations were observed in the simulation. To the best knowledge of the present authors, chemical reactivity of silica nanowires and their building blocks has never systematically been investigated in the literature.

In this paper, using the $(SiO_2)_6$ nanostructure as an example, we address the following two issues, how many structures (local minima) it can access in gas phase and how its reactivity behaviors look like during the process of dynamic evolution in the conformation space. For that purpose, we perform Born−Oppenheimer quantum molecular dynamics[11,12] simulations for 15 picoseconds at 3000 K for the silica nanostructure and then sample its trajectory profile to discover distinctive conformers. A total of 13 conformers were found, 7 of which have not previously been reported in the literature. With the help of reactivity indices from DFT,[13,14] we investigate the dynamic profile of a number of DFT reactivity indices such as HOMO/LUMO, chemical potential,[15] hardness,[16] electrophilicity index,[17,18] and electro/nucleofugality indices.[19−21] Correlated fluctuations between HOMO and LUMO and between chemical potential and hardness are observed. Electrophilicty and nucleo/electrofugality indices are found to change concurrently and drastically during the course of dynamic simulation, indicating that the $(SiO_2)_6$ nanostructure and its coexistent isomers can be exceedingly chemically reactive.

2. Methodological Background

The potential energy surface (PES) includes all the information needed to characterize structural and dynamical properties of a molecular system. Nevertheless, the multidimensional nature of PES for a system comprising a large number of degrees of freedom from electrons and nuclei prevents us from explicitly depicting it because of insurmountable numerical difficulties. A feasible way is a sampling approach of the conformation space properly propagated via classical or quantum mechanics in the

---

* Corresponding author. E-mail: shubin@email.unc.edu.
† Taizhou College.
‡ Hunan Normal University.
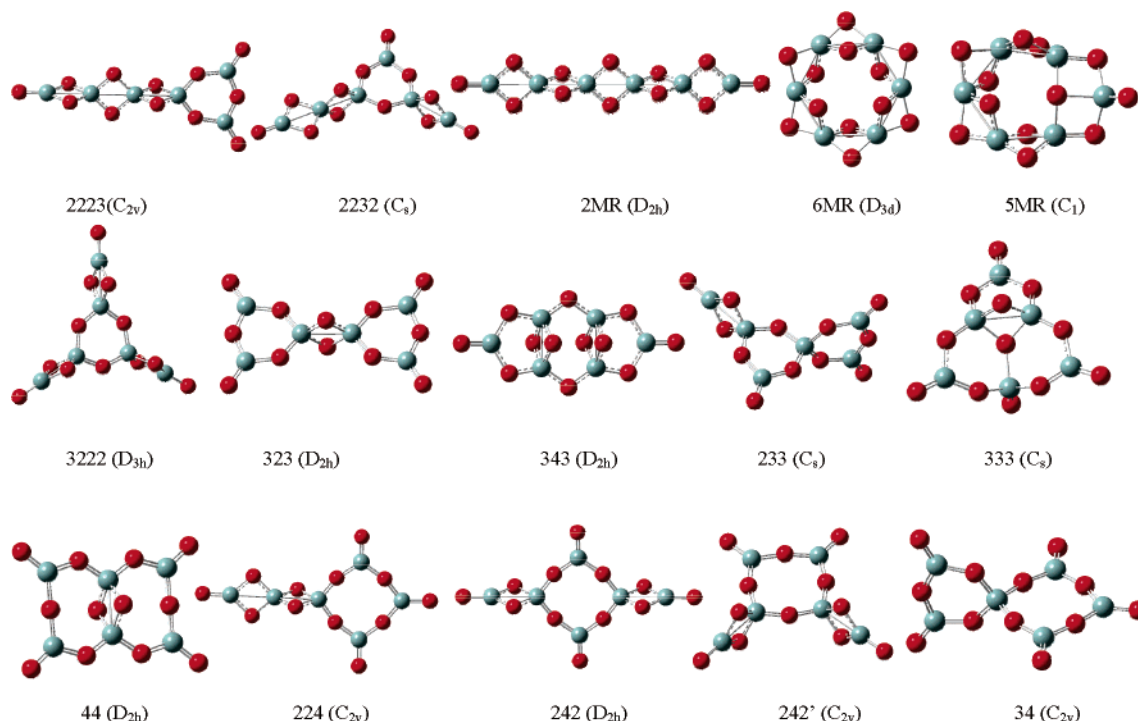§ University of North Carolina.

Figure 1. The optimized structure at the level of B3LYP/6-311+G(d) of 13 structures of (SiO₂)₆ nanostructures sampled from the BOMD simulation trajectories, plus 5MR and 6MR structures for the purpose of comparison.

space-time domain. Molecular dynamics, the numerical integration of the classical mechanical equation of motion governing the movement of atoms interacting on a multidimensional PES, is not suitable for systems such as the one of the present study where bond breaking and bond formation are taking place. For these processes, ab initio molecular orbital calculations have to be used directly to obtain the energies and derivatives, an approach called AIMD. A relatively new way of sampling molecular conformation space, AIMD is expanding rapidly in the past decade as high-performance computing hardware becomes more powerful and software more efficient. There are two AIMD categories: Born−Oppenheimer molecular dynamics (BOMD)[22,23] and extended Lagrangian molecular dynamics (ELMD) (e.g., Car−Parrinello molecular dynamics[24] and atom-centered density matrix propagation).[25] In the ELMD approach, both electrons and nuclei are treated as dynamic variables, whereas in BOMD nuclei are treated as Newtonian particles whose forces are from the fully converged electronic structure calculation in the Born−Oppenheimer approximation. Offering the advantage of propagating molecules on a well-defined PES, BOMD uses conventional ab inito or DFT methods, including Hartree−Fock, multi-configuration self-consistent-field, DFT, second-order Møller-Plesset perturbation theory, etc., to calculate the energy and gradients directly for electrons and employ velocity Verlet, leapfrog, or other predictor-corrector based algorithms as gradient-based methods to integrate the equations of motion for the nuclei. The gradient and Hessian from BOMD calculations provide a local quadratic approximation to the PES and the equations of motion can be integrated on this local surface in closed form, thus allowing significantly larger time steps (∼1 fs) in quantum molecular dynamic simulations.

   The energy component analysis has been used elsewhere[26−28] as a powerful tool to understand the physical nature of spin-related phenomena and will be employed in this study to determine if there is any dominant contribution from one or few energy components to dictate to the total energy difference

TABLE 1: Energy Component Analysis of the Relative Stability of Various Conformers of the (SiO₂)₆ Nanostructure[a]

conformer	ΔE_{tot}	ΔT_s	$\Delta E_{electrostatic}$	ΔE_{xc}	Δgap
3222	0.00	0.00	0.00	0.00	0.00
2MR	0.06	37.80	−21.12	−16.63	3.23
2232	3.27	0.93	2.32	0.02	−3.00
2223	6.88	−0.54	6.45	0.97	−6.92
233	9.18	−34.22	24.90	18.50	−8.30
44	10.37	−67.61	72.85	5.12	−12.22
323	14.01	−40.12	35.09	19.04	−9.45
333	16.82	−79.56	97.46	−1.08	−39.20
242	32.72	−56.85	64.06	25.50	−10.61
242	32.72	−56.85	64.06	25.50	−10.61
343	33.53	−85.37	169.64	−50.74	−29.06
224	37.49	−58.82	70.35	25.97	−14.76
34	43.02	−91.47	90.15	44.34	−15.68
5MR	96.15	−32.66	199.04	−70.23	−141.36
6MR	98.33	−59.20	209.66	−52.12	−34.59

[a] The last column shows the difference of the HOMO−LUMO gap. The global minimum is used as the reference. Units are kcal/mol.

among a series of local minima. In DFT,[13] the total energy difference between two structures, ΔE, can be expressed as[26−28]

$$\Delta E = \Delta T + \Delta E_{electrostatic} + \Delta E_{xc} \qquad (1)$$

where[28]

$$\Delta E_{electrostatic} = \Delta V_{nn} + \Delta J + \Delta V_{ne} \qquad (2)$$

and

$$\Delta E_{xc} = \Delta E_x + \Delta E_c \qquad (3)$$

where E, T, V_{ne}, V_{nn}, J, E_x, and E_c stand for the total energy, total kinetic energy, nuclear-electron attraction, nuclear−nuclear repulsion, classical Coulomb repulsion among electrons, exchange, and correlation energy, respectively. The reference structure is the global minimum from the present study.

DFT reactivity indices are conceptually insightful and practically convenient in predicting regioselectivity and understand reaction mechanisms.[14] We anticipate that they are equally important for and applicable to nanoscale systems to understand their reactivity. We use them to assess the chemical volatility of the concerned system. In DFT,[13] the chemical potential, μ, and chemical hardness, η, are defined as $\mu = -\chi = (\partial E/\partial N)_v$ and $\eta = (\partial^2 E/\partial N^2)_v = (\partial \mu/\partial N)_v$, where E is the total energy of the system, N is the number of electrons in the system, and v is the external potential. μ is identified as the negative of electronegativity (χ) by Iczkowski and Margrave.[29] According to Mulliken,[30] one has

$$\mu = -\chi = -\frac{1}{2}(I + A) \tag{4}$$

and according to Parr and Pearson[31]

$$\eta = I - A \tag{5}$$

where I and A are the first ionization potential and electron affinity, respectively. Under the Koopmans' theorem for closed-shell molecules, based on the finite difference approach, I and A can be expressed in terms of the highest occupied molecular orbital (HOMO) energy, ϵ_{HOMO}, and the lowest unoccupied molecular orbital (LUMO) energy, ϵ_{LUMO}, respectively

$$I \approx -\epsilon_{HOMO}; \quad A \approx -\epsilon_{LUMO} \tag{6}$$

Recently, Parr, Szentpaly, and Liu[17] introduced the concept of electrophilicity index, ω, in terms of μ and η

$$\omega = \frac{\mu^2}{2\eta} \tag{7}$$

appraising the capacity of an electrophile to accept the maximal number of electrons in a neighboring reservoir of electron sea. Very recently, Ayers and co-workers[19–21] have proposed two new reactivity indices to quantify nucleophilic

and electrophilic capabilities of a leaving group, nucleofugality ΔE_n and electrofugality ΔE_e, defined as follows:

$$\Delta E_n = -A + \omega = \frac{(\mu + \eta)^2}{2\eta} \tag{8}$$

$$\Delta E_e = I + \omega = \frac{(\mu - \eta)^2}{2\eta} \tag{9}$$

We will investigate in the present work how these quantities evolve during the course of the BOMD simulation.

3. Computational Details

An extensive review of the Born−Oppenheimer molecular dynamics method is available elsewhere.[11] In the implementation of QMD in the NWChem package,[32] both ab initio and DFT approaches are accessible for the quantum mechanic calculation. We performed BOMD simulations at the level of B3LYP/6-311G(d) for the building block of silica nanowire, $(SiO_2)_6$, according to the following protocol. After an initial structure optimization of 120 steps, the system is undergone quantum molecular dynamics simulations under 3000 K for 15 ps with a step size of 0.5 fs and the leapfrog integration algorithm. We employ a constant temperature ensemble using Berendsen's thermostat with the temperature relaxation time set to be 2 fs enabling the system to quickly reach equilibrium.[33] The cutoff radius for short range interactions is 2.8 nm. SHAKE is disabled and thus all bonding interactions are treated according to the force calculated from quantum mechanics. BOMD output and trajectories are saved in every 5 femtoseconds and are processed and analyzed aftermaths. As reported elsewhere[33] from the data of the temperature variation and the root-mean-square energy fluctuation for the potential and total energies, the dynamic system is stable and quickly reaches the equilibrium state. Postprocessing scripts are composed to extract HOMO/LUMO energies from the BOMD output and to search for distinctive conformations from the trajectories. Equations 4−9 are used to calculate the time profile for μ, η, ω, ΔE_n, and ΔE_e. For each of the candidate conformation extracted by the postprocessing script, a full geometrical optimization is performed at the level of B3LYP/6-311+G(d) using the Gaussian 03 package version
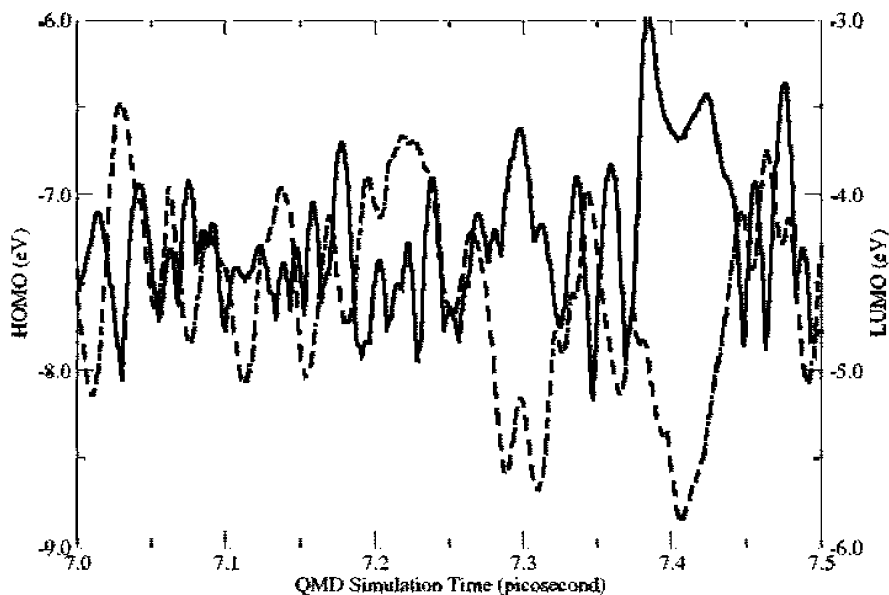

Figure 2. Sample time profiles of HOMO (solid line) and LUMO (dashed line) in the course of BOMD simulations.
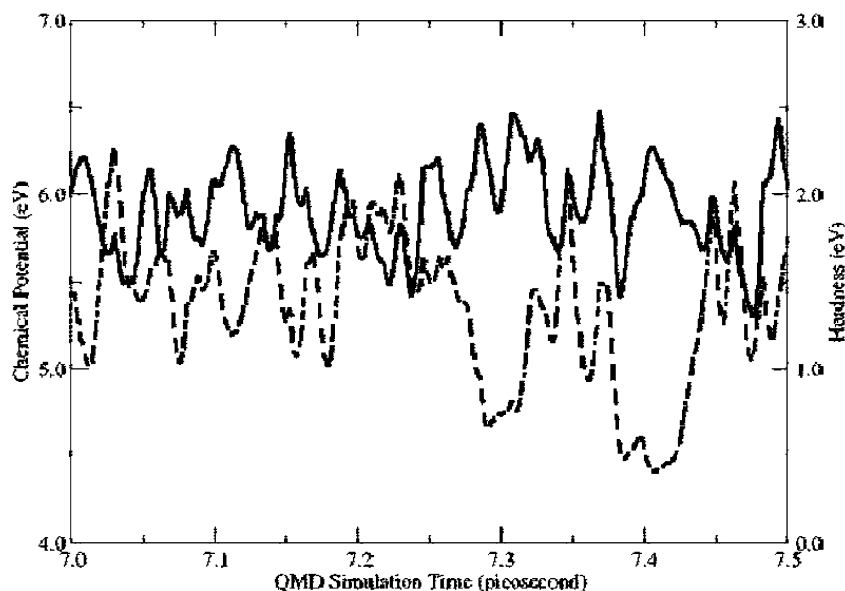
(SiO$_2$)$_6$ Silica Nanostructures

J. Phys. Chem. A, Vol. 111, No. 16, 2007 **3135**

Figure 3. Sample time profiles of chemical potential (solid line) and hardness (dashed line) in the course of BOMD simulations.

C02[34] with tight SCF convergence and ultra fine integration grids. An energy component analysis is conducted after the optimized structure is obtained.

4. Results and Discussion

Figure 1 displays a total of 13 (SiO$_2$)$_6$ nanostructures, 3222, 2MR, 2232, 2223, 233, 44, 323, 333, 242, 242′, 343, 224, and 34, discovered from the above procedures and encoded by the manner in which a structure is formed from 2MR, 3MR, and 4MR building blocks. Among the 13 structures, seven conformers, 2223, 2232, 323, 224, 242, 242′, and 34, have not previously been reported in the literature. Also included in the Figure are the 5MR and 6MR structures for the purpose of comparison, as is the point group for each of the structures. From the 13 local minima found in the BOMD simulation, we did not observe any structure with 5- or 6-membered ring, conforming earlier findings[5−10] that building blocks of silica nanostructures are indeed 2MR, 3MR, and/or 4MR.

To see if there is a dominant energy component contributing to the energy difference among the conformers, an energy component analysis has been conducted for them. Table 1 exhibits the result of the analysis, from which one finds that (i) consistent with the literature,[9] 3222 is the global minimum, (ii) the energy difference between 3222 and 2MR structures, 0.06 kcal/mol at the B3LYP/6-311+G(d) level, is negligibly small, (iii) the reason why 5MR and 6MR structures are not accessible is because they are thermodynamically too unstable, each with larger than 90 kcal/mol in energy than the global minimum, (iv) among the three terms considered in this work, ΔT, $\Delta E_{\text{electrostatic}}$, and ΔE_{xc}, there is no single component dictating the trend of all points of ΔE in the Table, and (v) except for 2MR and 2232 ΔT contributes negatively to ΔE of all conformers and except for 2MR $\Delta E_{\text{electrostatic}}$ contributes positively to ΔE. For ΔE_{xc}, its contribution is mixed, with some contributing positively and others negatively to ΔE. Generally speaking, as shown in the Table, it is the lower electrostatic interaction of the global minimum that differentiates it from the others. The only exception is the 2MR structure, where one finds that it is the lower kinetic component that plays the governing role.

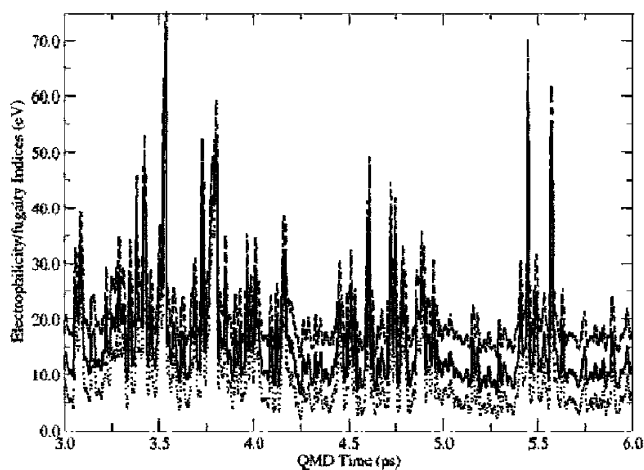Shown in the last column of Table 1 is the difference of the HOMO−LUMO gap between the global minimum and various

Figure 4. Sample time profiles of electrophilicity index (solid line), nucleofugality (dashed line), and electrofugality (dotted line) in the course of BOMD simulations.

local minima, from which one finds that except for the 2MR conformer, the HOMO−LUMO gap of the global minimum is larger than that of the local minima, confirming that, though not always true, the maximum hardness principle[14,35−38] is valid for this system and it is a useful conceptual framework from DFT to understand and rationalize molecular stability.

Figures 2−4 display portions of the time profile for a few DFT reactivity indices. Shown in Figure 2 are the dynamic behaviors of HOMO and LUMO for a span of 0.5 picoseconds during the BOMD simulation. It is observed from the Figure that HOMO fluctuates more quickly than LUMO[33] as evidenced by the total number of peaks for HOMO (27 peaks) and LUMO (14 peaks). Furthermore, there seemingly exists certain correlation in the pattern of the dynamic fluctuation between HOMO and LUMO: a peak in LUMO often, though not always, corresponds to a peak or valley in HOMO, and vise versa. The same coherence of dynamic behaviors shown in Figure 3 is also observed between the chemical potential and hardness computed by eqs 4−6. We notice that the coherent behavior between the chemical potential and hardness is a consequence of that of HOMO and LUMO through the approximation introduced in eq 6. These correlated dynamic behaviors of DFT reactivity indices have been reported elsewhere for other systems.[33]

Shown in Figure 4 are time profiles of three more recently defined DFT reactivity indices, electrophilicity index,[17,18] electrofugality, and nucleofugality.[19−21,39] From Figure 4, one finds that (i) these three indices fluctuate concurrently and (ii) they change drastically during the QMD simulation. The concurrent fluctuation pattern of these three indices comes from the fact that HOMO changes faster than LUMO and that the two frontier orbitals evolve coherently as demonstrated in Figure 2. The large alteration amplitude of electrophilicity index, electrofugality and nucleofugality indicates that as the local minima are sampled during the process the silica nanostructure can become exceedingly reactive and chemically volatile, providing possibilities for a variety of chemical modifications in admissible circumstances.

5. Conclusions

Born−Oppenheimer molecular dynamic simulations have been performed in this work for the nanostructure, $(SiO_2)_6$, to investigate its structural and dynamic properties. A total of 13 conformations have been identified, 7 of which have not previously been reported. Fundamental building blocks of silica nanostructures are confirmed to be 2-, 3-, and 4-member rings. The energy component analysis shows that even though there is no single dominant energy component dictating the energy difference between a given local minimum and the global structure, it is the lower electrostatic interaction that differentiates the global minimum from the others. We also observed that the maximum hardness principle could play a role in justifying the molecular stability of the system. Time profiles of a few DFT reactivity indices exhibit pattern correlations of dynamic fluctuations between HOMO and LUMO and between chemical potential and hardness. Electrophilicity index, nucleaofugality, and electrofugality are found to change concurrently and drastically during the dynamic simulation, demonstrating that the species are chemically volatile.

References and Notes

(1) Huang, M.; Mao, S.; Feick, H.; Yan, H.; Wu, Y.; Kind, H.; Weber, E.; Russo, R.; Yang, P. *Science* **2001**, *292*, 1897.

(2) Zhang, M.; Ciocan, E.; Bando, Y.; Wada, K.; Cheng, L. L.; Pirouz, P. *Appl. Phys. Lett.* **2002**, *80*, 491.

(3) Tong, L.; Gattass, R. R.; Ashcom, J. B.; He, S.; Lou, J.; Shen, M.; Maxwell, I.; Mazur, E. *Nature* **2003**, *426*, 816.

(4) Chen, J.-F.; Ding, H.-M.; Wang, J.-X.; Shao, L. *Biomaterials* **2004**, *25*, 723.

(5) Harkless, J. A. W.; Stillinger, D. K.; Stillinger, F. H. *J. Phys. Chem.* **1996**, *100*, 1098.

(6) Nayak, S. K.; Rao, B. K.; Khanna, S. N.; Jena, P. *J. Chem. Phys.* **1998**, *109*, 1245.

(7) Chu, T. S.; Zhang, R. Q.; Cheung, H. F. *J. Phys. Chem. B* **2001**, *105*, 1705.

(8) Flikkema, E.; Bromley, S. T. *J. Phys. Chem. B* **2004**, *108*, 9638.

(9) Zhang, D. J.; Zhang, R. Q. *J. Phys. Chem. B.* **2006**, *110*, 1338.

(10) Zhang, D.; Guo, G.; Liu, C.; Zhang, R. Q. *J. Phys. Chem. B* **2006**, *110*, 23633.

(11) Bolton, K.; Hase, W. L.; Peshlherbe, G. H. *Modern Methods for Multidimensional Dynamics Computation in Chemistry*; Thompson, D. L., Ed.; World Scientific: Singapore, 1998; p 143.

(12) Schlegel, H. B. *Bull. Korean Chem. Soc.* **2003**, *24*, 1.

(13) Parr, R. G.; Yang, W. *Density Functional Theory of Atoms and Molecules*; Oxford University Press: Oxford, 1989.

(14) Geerlings, P.; De Proft, F.; Langenaeker, W. *Chem. Rev.* **2003**, *103*, 1793.

(15) Parr, R. G.; Donnelly, R. A.; Levy, M.; Palke, W. E. *J. Chem. Phys.* **1978**, *68*, 3801.

(16) Parr, R. G.; Pearson, R. G. *J. Am. Chem. Soc.* **1983**, *105*, 7512.

(17) Parr, R. G.; Szentpaly, L. V.; Liu, S. B. *J. Am. Chem. Soc.* **1999**, *105*, 1922.

(18) For, a review, see Chattaraj, P. K.; Sarkar, U.; Roy, D. R. *Chem. Rev.* **2006**, *106*, 2065.

(19) Ayers, P. W.; Anderson, J. S. M.; Rodriguez, J. I.; Jawed, Z. *Phys. Chem. Chem. Phys.* **2005**, *7*, 1918.

(20) Ayers, P. W.; Anderson, J. S. M.; Bartolotti, L. J. *Int. J. Quantum Chem.* **2005**, *101*, 520.

(21) Roos, G.; Loverix, S.; Brosens, E.; Van Belle, K.; Wyns, L.; Geerlings, P.; Messens, J. *ChemBioChem* **2006**, *7*, 981.

(22) Helgaker, T.; Uggerud, E.; Jensen, H. J. A. *Chem. Phys. Lett.* **1990**, *173*, 145.

(23) Chen, W.; Hase, W. L.; Schlegel, H. B. *Chem. Phys. Lett.* **1994**, *228*, 436.

(24) Car, R.; Parrinello, M. *Phys. Rev. Lett.* **1985**, *55*, 2471.

(25) Schlegel, H. B.; Iyengar, S. S.; Li, X.; Millam, J. M.; Voth, G. A.; Scuseria, G. E.; Frisch, M. J. *J. Chem. Phys.* **2002**, *117*, 8694.

(26) Liu, S. B.; Langenaeker, W. *Theor. Chem. Acc.* **2003**, *110*, 338.

(27) Zhong, A. G.; Liu, S. B. *J. Theor. Comp. Chem.* **2005**, *4*, 833.

(28) Rong, C.; Lian, S.; Yin, D.; Shen, B.; Zhong, A. G.; Bartolotti, L.; Liu, S. B. *J. Chem. Phys.* **2006**, *125*, 174102.

(29) Iczkowski, R. P.; Margrave, J. L. *J. Am. Chem. Soc.* **1961**, *83*, 3547.

(30) Mulliken, R. S. *J. Chem. Phys.* **1934**, *2*, 782.

(31) Ayers, P. W.; Parr, R. G.; Pearson, R. G. *J. Chem. Phys.* **2006**, *124*, 194107.

(32) Aprà E. et al NWChem. *A Computational Chemistry Package for Parallel Computers*, version 4.7; Pacific Northwest National Laboratory: Richland, WA, 2005.

(33) Liu, S. B. *J. Chem. Sci.* **2005**, *117*, 477.

(34) Frisch M. J. et al., *Gaussian 03*, Revision C.02; Gaussian, Inc.: Pittsburgh, PA, 2003.

(35) Pearson, R. G. *Chemical Hardness*; Wiley-VCH: Weinheim, Germany, 1997.

(36) Pearson, R. G. *J. Chem. Educ.* **1968**, *45*, 981.

(37) Pearson, R. G. *Acc. Chem. Res.* **1993**, *26*, 250.

(38) Pearson, R. G. *J. Chem. Educ.* **1999**, *76*, 267.

(39) Rong, C.; Lian, S.; Yin, D.; Zhong, A. G.; Zhang, R. Q.; Liu, S. B. *Chem. Phys. Lett.* **2006**, *434*, 149.